Peer-reviewed version available at *Int. J. Mol. Sci.* **2017**, *18*, 2081; doi:10.3390/ijms18102081

Article

Omega-3 Polyunsaturated Fatty Acids Protect Against Ischemia-Reperfusion Renal Injury Through AMPK-Mediated Autophagy

Do Hyeong Gwon[1,†], Tae Woong Hwang[1,†], Ju-ye Ro[2], Yoon-Joong Kang[3], Jin Young Jeong[4,5], Do-Kyung Kim[6], Kyu Lim[7], Dong Woon Kim[1,8], Dae Eun Choi[4,*], and Jwa-Jin Kim[1,3,5,8,*]

[1] Department of Anatomy, School of Medicine, Chungnam National University, Daejeon 301-747, South Korea; dohyeong171@gmail.com (D.H.); dkdnwl1234@gmail.com (T.W.); visnu528@cnu.ac.kr (D.W.); kjj4827@gmail.com (J.J.)

[2] Department of Biomedical Laboratory Science, College of Medical Science, Konyang University, Daejeon 302-718, South Korea; chamas89@gmail.com (J.Y.)

[3] Department of Biomedical Science, Jungwon University, Geosan, Chungbuk 367-805, South Korea; yjkang@jwu.ac.kr (Y.J.); kjj4827@gmail.com (J.J.)

[4] Department of Nephrology, School of Medicine, Chungnam National University, Daejeon,, South Korea; spwlsdud@naver.com (J.Y.); daenii@naver.com (D.E.)

[5] Department of Medical Science, School of Medicine, Chungnam National University, Daejeon,, South Korea; spwlsdud@naver.com (J.Y.); kjj4827@gmail.com (J.J.)

[6] Department of Anatomy, College of Medicine, Konyang University, Daejeon, South Korea; dokyung@konyang.ac.kr (D.K.)

[7] Department of Biochemistry, School of Medicine, Chungnam National University, Daejeon 301-747, South Korea; kyulim@cnu.ac.kr (K.)

[8] Brain Research Institute, School of Medicine, Chungnam National University, Daejeon 301-747, South Korea; chamas89@gmail.com (J.Y.); visnu528@cnu.ac.kr (D.W.); kjj4827@gmail.com (J.J.)

* Correspondence: kjj4827@gmail.com; Tel.: +82-42-580-8210, daenii@naver.com; Tel.: +82-42-280-8374

† These authors contributed equally to this work.

Abstract: Regulated autophagy is involved in the repair of renal ischemia-reperfusion injury (IRI). ω3-Polyunsaturated fatty acids (ω3-PUFAs) show protective effects against various renal injuries. It was recently reported that ω3-PUFAs regulate autophagy. We assessed whether ω3-PUFAs attenuated IR-induced acute kidney injury (AKI) and evaluated associated mechanisms. C57Bl/6 background fat-1 mice and wild-type mice (wt) were divided into four groups: wt sham (n = 10), fat-1 sham (n = 10), wt IRI (reperfusion 35 min after clamping both the renal artery and vein; n = 15), and fat-1 IRI (n = 15). Kidneys and blood were harvested 24 h after IRI. Renal histological and molecular data were collected. The kidneys of fat-1 mice showed better renal cell survival, renal function, and pathological damage than those of wt mice after IRI. In addition, fat-1 mice showed less oxidative stress and autophagy impairment; greater amounts of LC3, Beclin-1, and Atg7; lower amounts of p62; and higher levels of renal cathepsin D and ATP6E than wt kidneys. They also showed more AMPK activation, which resulted in the inhibition of phosphorylation of the mammalian target of rapamycin (mTOR). Collectively, ω3-PUFAs in fat-1 mice contributed to AMPK mediated autophagy activation, leading to a renoprotective response.

Keywords: ischemia-reperfusion injury (IRI), ω3-PUFA, AMP-activated protein kinase (AMPK), autophagy

1. Introduction

Although there are many causes of acute renal dysfunction, renal ischemic and/or reperfusion injuries are a major cause of acute kidney injury in renal transplantation [1]. Complex mechanisms are involved in ischemia-reperfusion injury (IRI). Hypoxic injury triggers the tubular cell secretion of

Peer-reviewed version available at Int. J. Mol. Sci. 2017, 18, 2081; doi:10.3390/ijms18102081

cytokines associated with acute inflammatory processes, the generation of reactive oxygen species (ROS), and apoptotic and necrotic cell death [2-4]. Moreover, reperfusion following ischemia generates large amounts of ROS, resulting in tubular cell death [5]. Recent studies have shown that oxidative stress and associated autophagy signaling play important roles in renal IRI [6,7].

Autophagy has recently been found to be an important regulator in adaptive cellular and tissue responses to IRI [8]. Although autophagy serves as a housekeeping process, maintaining homeostasis under physiological conditions [7], dysregulated and particularly excessive autophagy may be devastating under pathological conditions, such as in dilated cardiomyopathy, alcoholic cardiomyopathy, myocardial hypertrophy, and heart failure [9-11].

Recent reports have suggested that the activation of autophagy attenuates IRI of the kidney [8]. However, to date, the precise role of autophagy and the underlying regulatory mechanisms remain unclear with regard to IR-induced renal anomalies. Many regulators of autophagy have been implicated, including ATG1, mTOR, and AMP-activated protein kinase (AMPK) [12]. AMPK, in particular, is considered a potentially important regulator of autophagy in the kidney [13]. It is rapidly phosphorylated in ischemic tubular cells [14]. It has also been reported that AICAR (an AMPK agonist) is increased in LC3 puncta, a marker of autophagy, resulting in attenuated renal IRI [14].

Studies have shown that ω3-PUFAs can protect against ischemic injury [15]. Indeed, significant concentrations of ω3-PUFAs are present in many human tissues [16], and are significantly involved in reducing ROS and attenuating ischemic acute renal failure [17]. Furthermore, ω3-PUFAs increase the phosphorylation of AMPK in ischemic intestines [18]. The energy-sensing LKB1-AMPK pathway regulates cell survival under energy-deprivation conditions, increasing the AMP:ATP ratio [19]. Moreover, AMPK has been implicated in many aspects of cell proliferation, apoptosis, and autophagy [20-22]. Furthermore, ω3-PUFAs are involved in modulating autophagy via Akt-mTOR signaling in prostate cancer and lung cancer [22,23]. These reports suggest that ω3-PUFAs may regulate autophagy activation via the AMPK pathway in IR-induced kidneys.

Fat-1 transgenic mice express a Caenorhabditis elegans ω3 desaturase (fat-1), leading to endogenous synthesis of ω3-PUFAs from ω6-PUFAs. Fat-1 mice show not only enhanced concentrations of n-3 α-linolenic acid, eicosapentaenoic acid, docosahexaenoic acid, and docosapentaenoic acid, but also significantly reduced n-6 linoleic and arachidonic acids in muscle, red blood cells, heart, brain, liver, kidney, lung, and spleen tissues [24]. Despite this marked change in the ratio of n-6 to n-3, such transgenic mice are apparently normal and healthy. Thus, this model is ideal for studying the effects of the tissue n-6/n-3 ratio in the body.

In this study, we demonstrate the effects of ω3-PUFAs on IR-induced AKI. Importantly, ω3-PUFAs appear to be involved in a renoprotective mechanism for cell survival.

2. Results

2.1. Effects of endogenous ω3-PUFAs on renal function

To evaluate renal function, BUN and serum creatinine were measured. Levels of BUN and serum creatinine were significantly higher in wt IRI mice than in wt sham mice (Fig. 1A, B). They were also significantly higher in fat-1 IRI mice than in fat-1 sham mice, and in wt IRI mice than in fat-1 IRI mice.

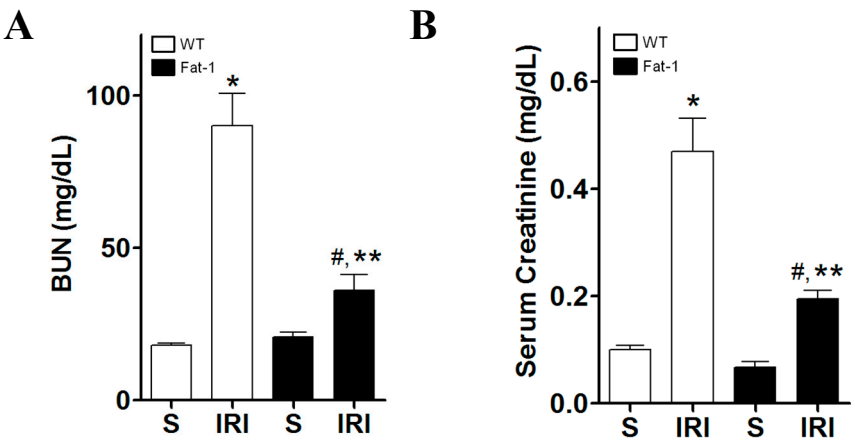

Figure 1. Effects of ω3-PUFA on renal function. Effect of fat-1 induction on renal function in ischemia reperfusion (IR) renal injury mice (WT-S, wild type sham; WT-IRI, IR renal injury in wild-type mice; fat-1, fat-1 induction sham; fat-1 IRI, IR renal injury in fat-1 induction mice). The levels of (A) BUN and (B) serum creatinine were significantly increased in wt IRI mice compared to sham mice. Fat-1 IRI mice showed decreased the levels of BUN and serum creatinine, compared to wt IRI mice. *P < 0.05 vs.WT sham kidney, #P < 0.05 vs. fat-1 sham kidney, ** P < 0.05 vs.WT IRI kidney. Bar represents mean ± s.d.

2.2. Effects of endogenous ω3-PUFAs on renal tissue injury

To evaluation renal tissue damage, H&E and PAS staining were performed. In H&E-stained cells, tubular cell necrosis and flattening and interstitial inflammation were observed in wt IRI mice. Tubulointerstitial injury scores were significantly higher in wt IRI mice than in wt sham mice. Fat-1 IRI mice had significantly lower tubulointerstitial injury scores than wt IRI mice (Fig. 2A, B). In PAS-stained cells, tubular necrosis, vacuolization, flattening, and loss of brush borders were observed in wt IRI mice. Fat-1 IRI mice had significantly lower tubular injury scores than wt IRI mice (Fig. 2C, D). Further examination of renal tissues using the TUNEL assay showed that fat-1 tubular cells did not undergo apoptosis with IR (Fig. 2E). Western blot results showed that levels of the apoptotic marker cleaved caspase-3 were significantly higher in wt mice after IRI than in wt sham mice. H

owever, renal levels of cleaved caspase-3 were significantly lower in fat-1 IRI mice versus wt IRI mice. Although fat-1 IRI mice had slightly higher cleaved caspase-3 levels than fat-1 sham mice, the difference was not significant (Fig. 2F). These results suggest that enrichment of ω3-PUFAs may function as a negative regulator of apoptosis and may protect renal cells from death induced by IRI.

Peer-reviewed version available at Int. J. Mol. Sci. 2017, 18, 2081; doi:10.3390/ijms18102081

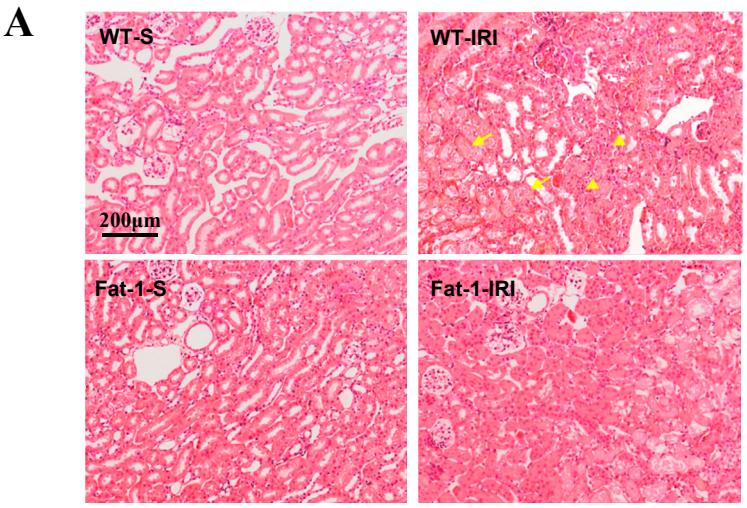

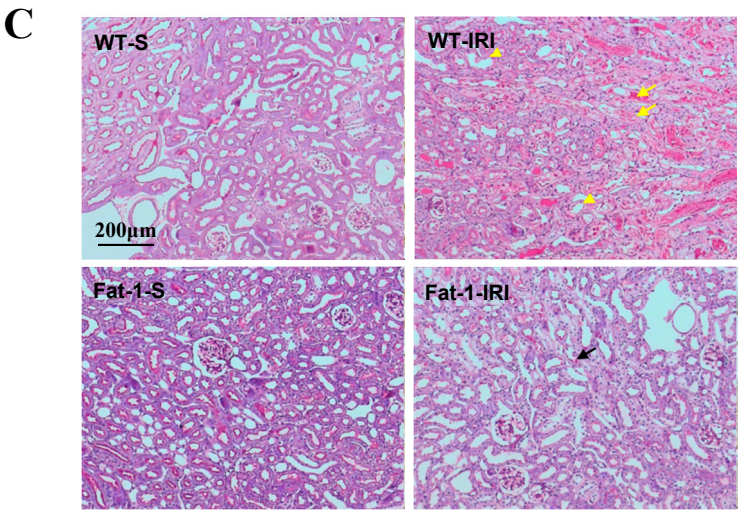

Preprints (www.preprints.org) | NOT PEER-REVIEWED | Posted: 4 August 2017 doi:10.20944/preprints201708.0015.v1

Peer-reviewed version available at Int. J. Mol. Sci. 2017, 18, 2081; doi:10.3390/ijms18102081

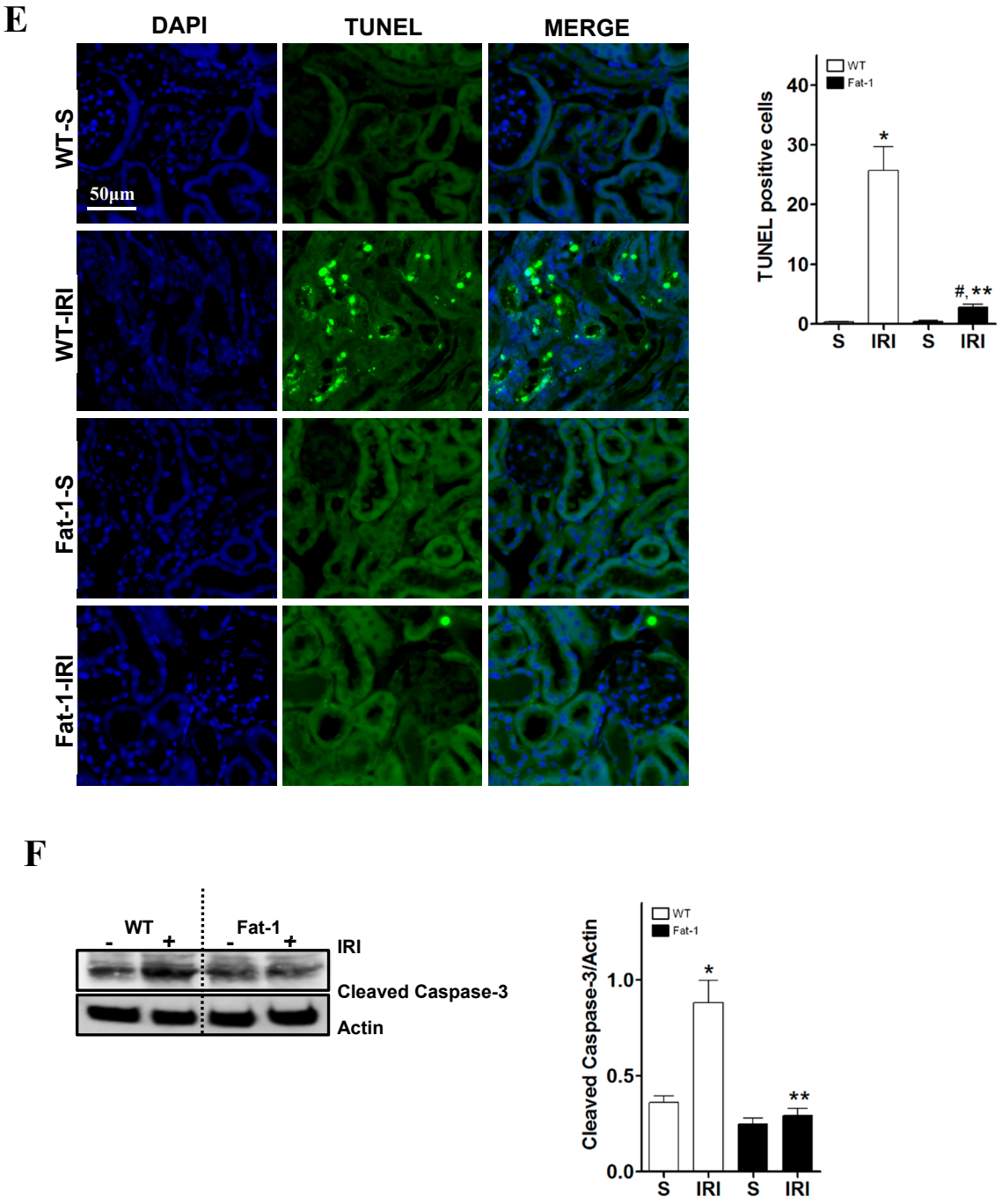

Figure 2. Effect of ω3-PUFA on renal histology and apoptosis in IR kidney. Representative kidney section stained with PAS and H&E (WT-S, wild type sham; WT-IRI, IR renal injury in wild-type mice; fat-1, fat-1 induction sham; fat-1 IRI, IR renal injury in fat-1 induction mice). (A) PAS stain; yellow arrows indicate necrotized tubules or cast formation. Yellow arrowheads indicate loss of brush border or dilated tubules. Black arrow indicates brush border. Original magnification, 200x. Scale bar = 200 μm. (B) A semi-quantitative analysis of tubular injury in wild-type and fat-1induction mice kidneys 24 h after IR renal injury (n=5/each group). (C) H&E stain; yellow arrows indicate necrotized tubules. Yellow arrowheads indicate inflammatory cells. Original magnification, 200x. Scale bar = 200 μm. (D) A semiquantitative analysis of tubule interstitial injury in wild-type and fat-1 induction mice kidneys 24 h after IR renal injury (n=5/each group). (E) Representative TUNEL stain of kidney section. Original magnification, 400x. Quantification of TUNEL positive cells. Scale bar = 50 μm. (F) Representative western blot and quantification of densitometry of caspase-3. *P < 0.05 vs. WT-sham kidney, #P < 0.05 vs. fat-1-sham kidney, ** P < 0.05 vs.WT-IR kidney. Bar represents mean ± s.d.

Peer-reviewed version available at Int. J. Mol. Sci. 2017, 18, 2081; doi:10.3390/ijms18102081

2.3. Effects of endogenous ω3-PUFAs on oxidative stress

Although ischemic events alone may lead to tubular cell necrosis in the kidney, reperfusion, occurring upon restoration of blood flow, is associated with the production of ROS, which is considered to play an important role in reperfusion injury [28]. In our study, after verifying oxidative stress in proximal tubules under IR-induced conditions, ROS formation was measured with DCFH DA (Fig. 3A) and DHE fluorescence (Fig. 3B), as reliable markers of ROS in the kidney. ROS were detected in some proximal tubular cells of wt renal tissues during IRI, although this was barely apparent in fat-1 renal tissues. ROS production was significantly greater in wt IRI kidneys than in the control group. However, there was significantly lower fluorescence intensity in kidneys of fat-1 IRI mice than in wt IRI mice. Although fluorescence intensities were slightly higher in fat-1 IRI mice than in fat-1 sham mice, there were no significant differences in the levels of cleaved caspase-3 between these two groups. The role of ω3-PUFA was determined in terms of ROS-scavenging effects in fat-1 mice via the downregulation of p22phox (Fig. 3C). The mitochondrial anion carrier protein uncoupling protein 2 (UCP2) is key for modulating ROS production and inflammatory responses [29]. Hence, an increase in UCP2 may act as a protective response against oxidative stress, limiting the production of ROS. As shown in Figure 3D, in response to IRI, fat-1 kidney tissues showed an upregulation of mitochondrial UCP2; as a result, p22phox expression subsequently decreased. Thus ω3-PUFAs appeared to be involved in the regulation of UCP2, and p22phox expression resulted in enhanced antioxidant effects.

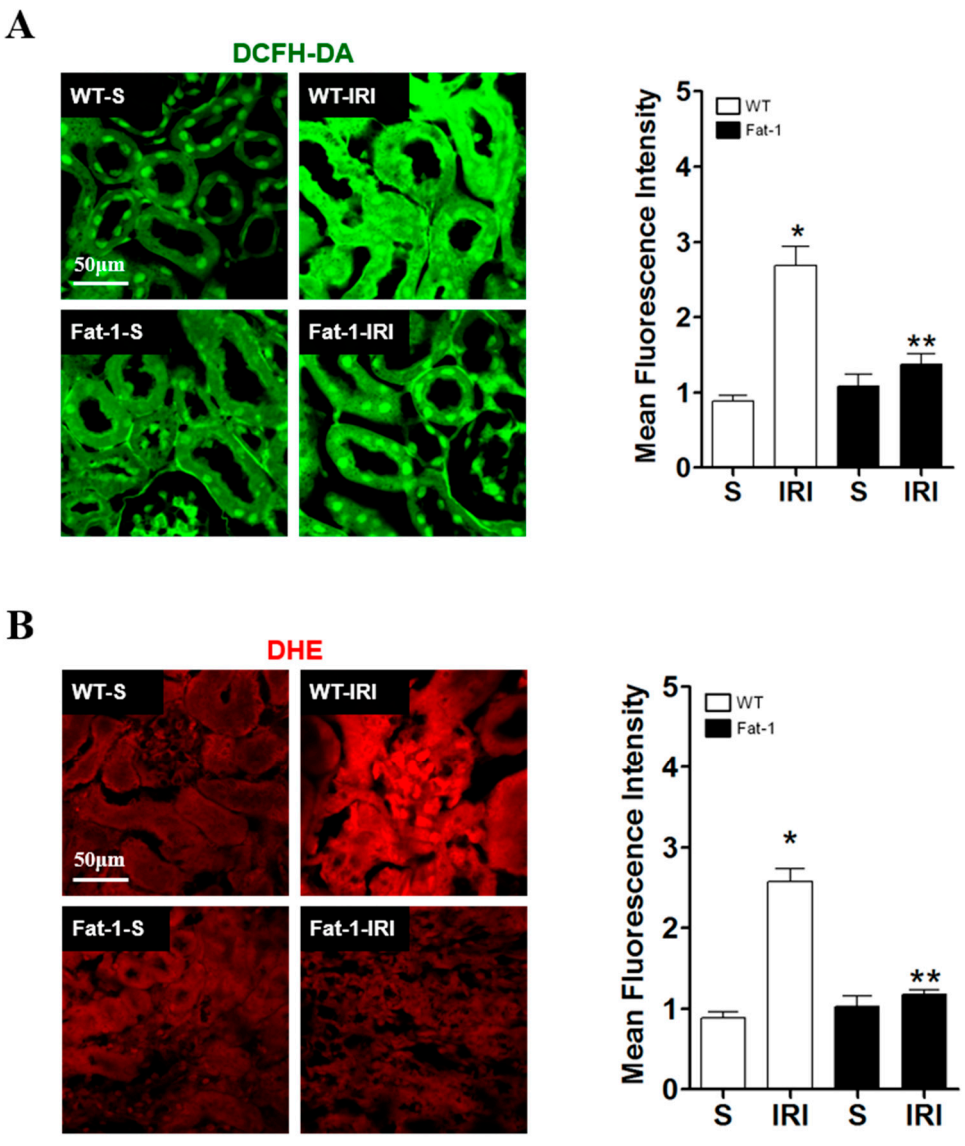

Preprints (www.preprints.org) | NOT PEER-REVIEWED | Posted: 4 August 2017 doi:10.20944/preprints201708.0015.v1

Peer-reviewed version available at Int. J. Mol. Sci. 2017, 18, 2081; doi:10.3390/ijms18102081

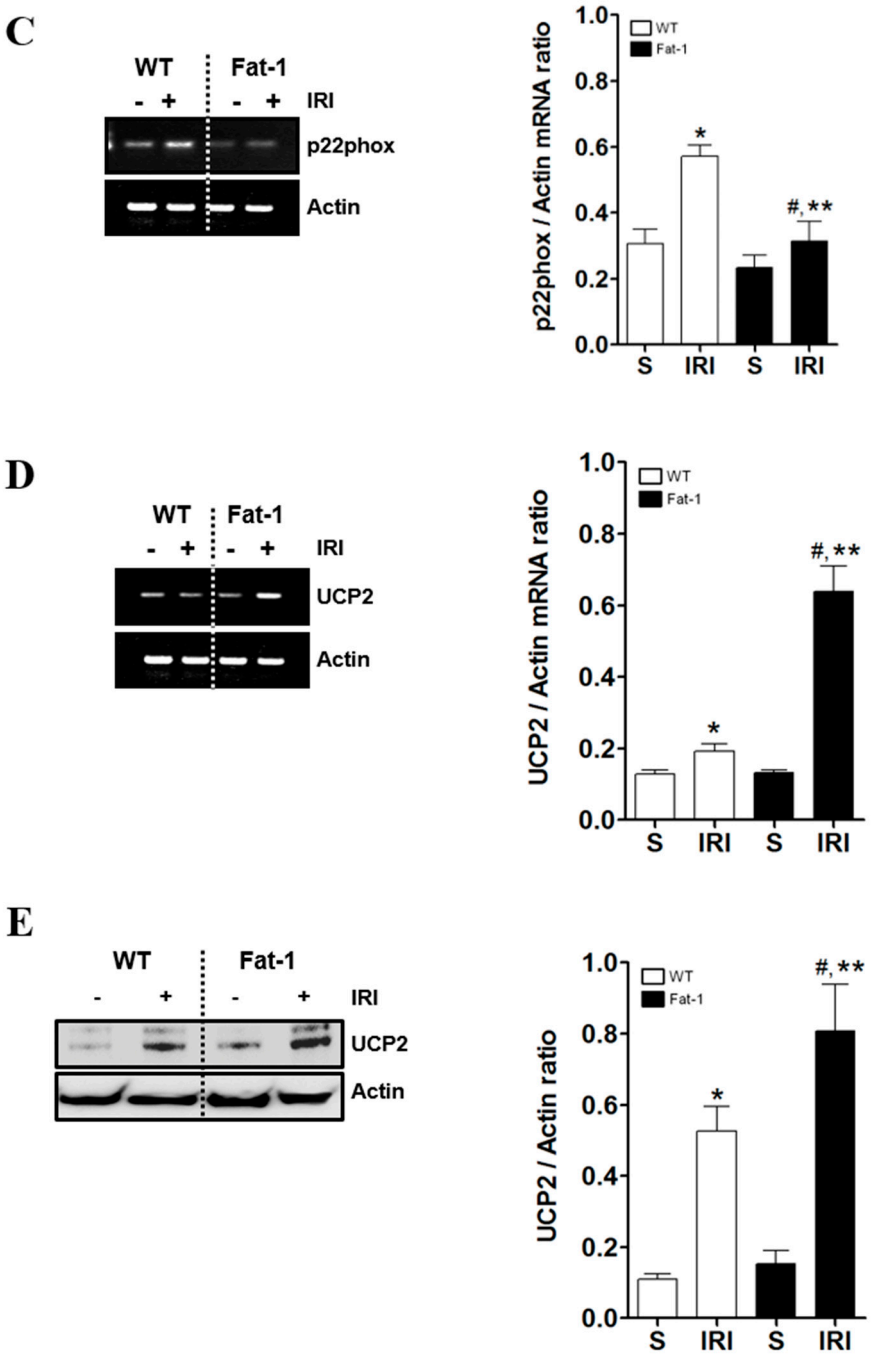

Figure 3. Effects of ω3-PUFA on oxidative stress in IR kidney. (A, B) Representative kidney section of ROS generation in mouse. (WT-S, wild type sham; WT-IRI, IR renal injury in wild-type mice; fat-1, fat-1 induction sham; fat-1 IRI, IR renal injury in fat-1 induction mice) (A) DCFH2-DA staining, detection of H_2O_2. Scale bar = 50 μm (B) DHA staining, detection of O_2 production. fat-1 IR mice kidney showed decreased fluorescence intensity of DCFH-DA and DHA compared to wild type IR mice kidney. Scale bar = 50 μm. (C, D) RT–PCR detection of p22phox and UCP2 mRNA expression in mouse tissues. Data were normalized using β-actin mRNA. Each bar graph, quantification. (E) Evaluation of anti-UCP2 antibody by immunoblot analysis. Left panel: whole tissue lysates from wild and transgenic fat-1 mice were electrophoresed and immunoblotted with anti-UCP2 antibody. Right panel: quantification of densitometry. Data were normalized using actin. *P < 0.05 vs.WT-sham kidney, #P < 0.05 vs. fat-1-sham kidney, ** P < 0.05 vs.WT-IR kidney. Bar represents mean ± s.d.

2.4. Effects of endogenous ω3-PUFAs on autophagy flux

A potential role of autophagy in kidney function and survival has been reported [30]. Progressive autophagy dysfunction can stimulate apoptosis and degeneration in renal cells in IR-induced AKI animals [7]. Thus, the enrichment effects of ω3-PUFAs on autophagy were investigated. First, immunofluorescence was examined with anti-LC3 in autophagy after inducing IRI. As shown in Figure 4, levels of microtubule-associated protein 1A/1B-light chain (LC3) were higher in wt IRI mice compared to a control group. These results suggest that autophagosome formation was increased after reperfusion in IRI-induced AKI wt mice (Fig. 4A). However, there was significantly more autophagosome formation in fat-1 mice than in wt IRI mice, as confirmed by assessing Beclin-1 and Atg7, known regulators of autophagy (Fig. 4B). Next, the level of sequestosome 1 (SQSTM1)/p62, also associated with autophagic flux, was examined, because it is involved in the dynamic process of the delivery of autophagic substrates to the lysosome and degradation of autophagic substrates inside the lysosome, and it may be a more reliable indicator of autophagic activity than measurements of autophagosomes. An accumulation of p62 was observed after IR-induced AKI due to autophagy flux blocking in wt IRI mice. Based on these results, the enrichment of ω3-PUFAs would seem to enhance the induction and flux of autophagy. However, the most important molecules in the maturation of autophagosomes/endosomes (such as cathepsin D and ATP6E, which are required for autophagosome–lysosome fusion) are essential for autophagosome clearance and autophagic flux [31]. The impact of n-3 fatty acids on autophagy flux in renal tissues was investigated. The levels of cathepsin D and ATP6E proteins were increased in IRI-induced AKI fat-1 mice, as shown by immunoblotting (Fig. 4C). Immunofluorescence staining was performed using LAMP1, a lysosomal marker. The colocalization of LC3 and LAMP1, induced by autophagy flux, was examined by confocal laser scanning microscopy (CLSM); it was higher in IRI-induced AKI fat-1 mice than in IRI-wt mice (Fig. 4D). Thus, ω3-PUFAs enhanced autophagy flux by increasing ATP6E and cathepsin D.

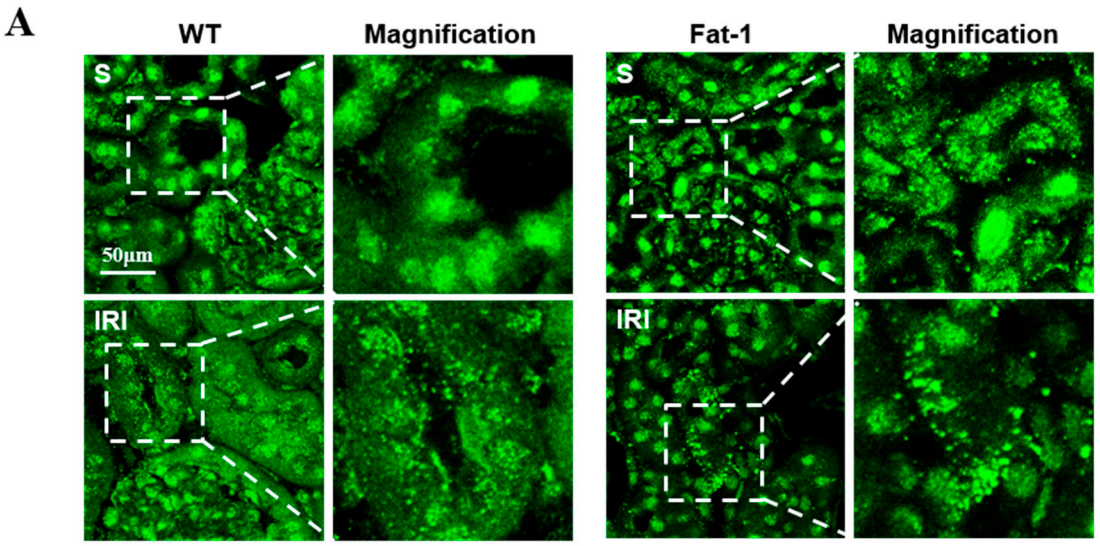

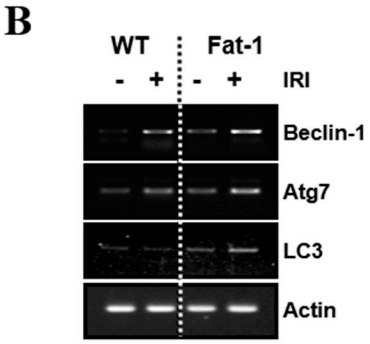

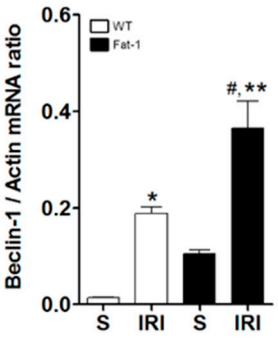

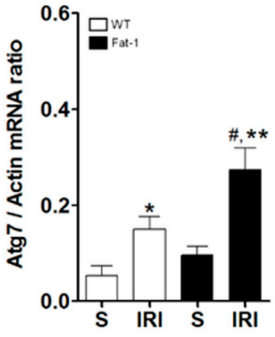

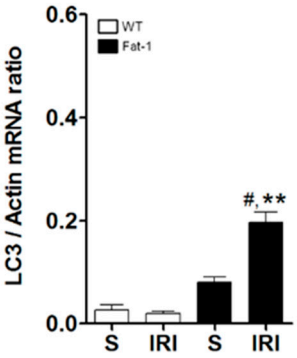

Preprints (www.preprints.org) | NOT PEER-REVIEWED | Posted: 4 August 2017 doi:10.20944/preprints201708.0015.v1

Peer-reviewed version available at Int. J. Mol. Sci. 2017, 18, 2081; doi:10.3390/ijms18102081

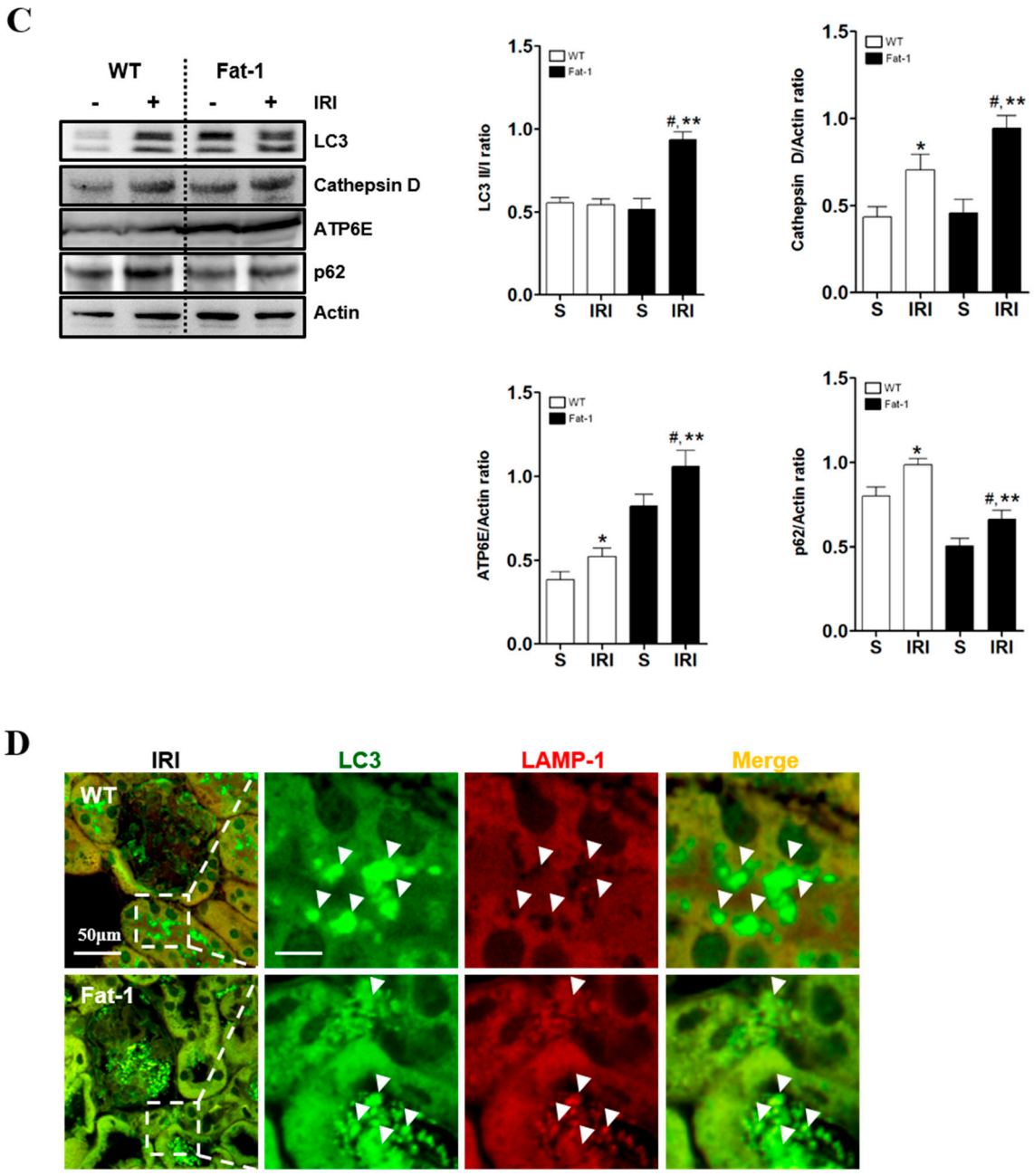

Figure 4. Effects of ω3-PUFA on autophagy flux in IR kidney. ω3-PUFA increased autophagy flux in fat-1 mice. (A) ω3-PUFA increases GFP–LC3-II accumulation and the appearance of punctate GFP-LC3 staining. Scale bar = 50 μm. (B) Total RNA of tissue following individual experiments was isolated and subjected to RT-PCR. Transcripts of Beclin-1, Atg7, and LC3 were examined after optimization of PCR conditions. Relative mRNA ratios of each autophagy-related gene are described relative to levels of actin. (C) Tissue proteins were immunoblotted with anti-LC3, anti-cathepsin D, ATP6E, and anti-p62. Immunoblotting with actin was performed as a loading control. Right bar graph indicates the ratios of LC3B-II/I and cathepsin D, ATP6E, and p62/actin as determined by densitometry. (D) Wild and transgenic fat-1 mouse were analyzed by fluorescent staining with LC3 and LAMP-1 to evaluate colocalization of LAMP1-positive lysosomes with LC3-labelled autophagosomes. The colocalization of punctate LC3 and LAMP 1 was assayed using confocal microscopy. Cell nucleus was stained with Hoechst (blue). Scale bar = 50 μm. *P < 0.05 vs.WT-sham kidney, #P < 0.05 vs. fat-1-sham kidney, ** P < 0.05 vs. WT-IR kidney. Bar represents mean ± s.d.

2.5. Effects of endogenous ω3-PUFAs on AMPK signaling

Because ω3-PUFAs induce autophagy and renoprotective responses and AMPK activity is regulated by the reversible phosphorylation of Thr172 of the catalytic α-subunit of AMPK, we determined whether AMPK activation by ω3 enrichment involved the inhibition of IR-mediated mTOR activation [32].

Based on the established role of AMPK in autophagy, via inhibition of mTOR [12], we hypothesized that ω3 enrichment-induced AMPK activation and subsequent mTOR inhibition may contribute to the induction of autophagy. To assess this, we first confirmed the phosphorylation of AMPK at Thr172 in IRI, measured by RT-PCR and Western blot. Kidneys were harvested at 12 h (RT-PCR) or 24 h (Western blot) after IRI. The rate of phosphorylated AMPK expression was 50% higher in fat-1 IRI mice than in wt IRI mice (Fig. 5A, B). That is, ω3 enrichment essentially amplified AMPK phosphorylation under normal conditions in fat-1 mice.

A previous study showed that IRI in kidneys increases activation of the mTOR-RPS6KB1/S6K1 (ribosomal protein S6kinase, 70 kDa, polypeptide 1) pathway [33]. Thus, we further examined the effects of ω3-PUFAs on mTOR phosphorylation in kidneys with IRI. In wt IRI mice, it significantly increased at Ser 2448 within 24 h compared to fat-1 IRI mice (Fig. 5C). Thus, ω3 enrichment in fat-1 mice decreased the IR induced phosphorylation of mTOR in the kidney. Our findings indicate that ω3-PUFA-induced AMPK activation may overcome mTOR activation during IRI, leading to renoprotective effects.

Preprints (www.preprints.org) | NOT PEER-REVIEWED | Posted: 4 August 2017 doi:10.20944/preprints201708.0015.v1

Peer-reviewed version available at Int. J. Mol. Sci. 2017, 18, 2081; doi:10.3390/ijms18102081

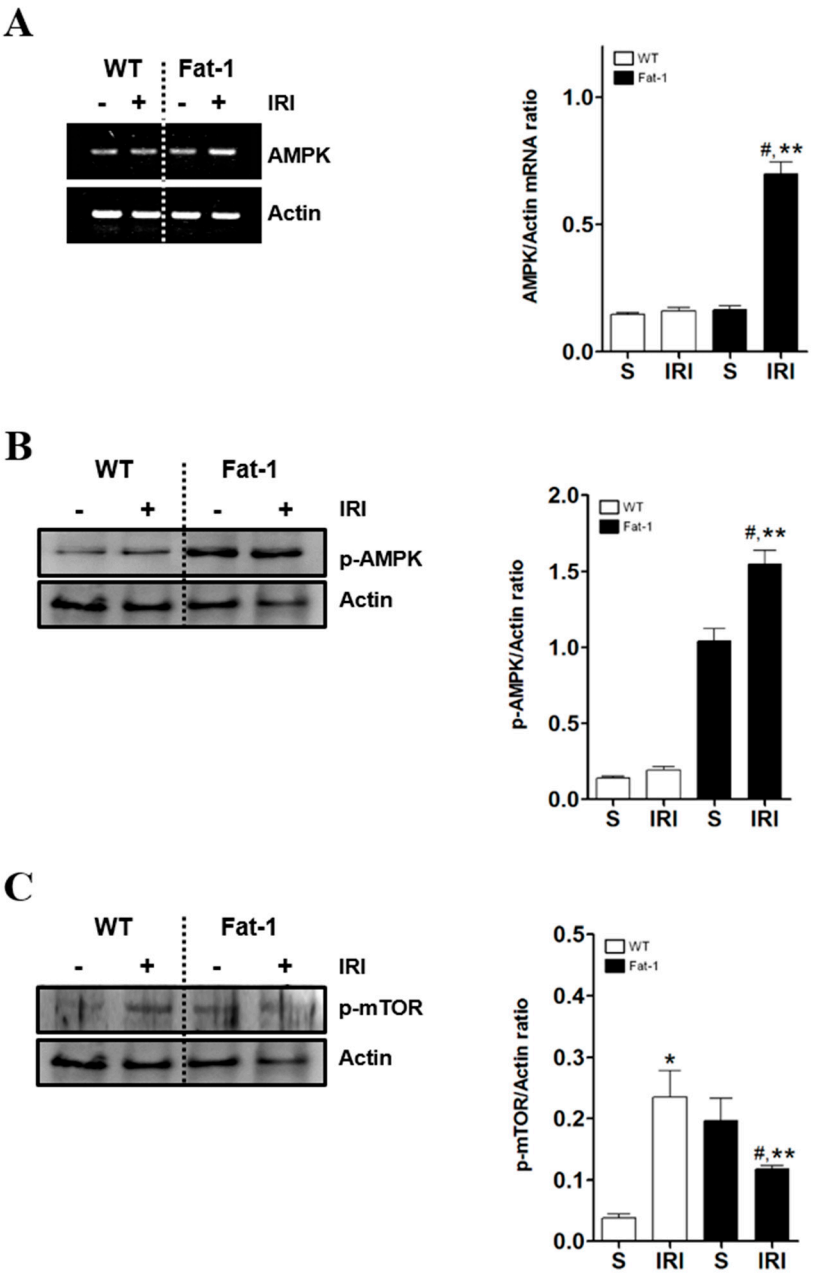

Figure 5. Effects of ω3-PUFA on AMPK and mTOR expression in IR kidney. Renal expression of AMPK and mTOR. (A) Representative picture and densitometry analysis of RT-PCR of AMPK in kidney tissue. (B) Representative picture and densitometry analysis of western blot of p-AMPK in kidney tissue. (C) Representative picture and densitometry analysis of mTOR in kidney section. Right panel: quantification of densitometry (n=7~8). Data were normalized using actin. *P < 0.05 vs.WT-sham kidney, #P < 0.05 vs. fat-1-sham kidney, ** P < 0.05 vs.WT-IR kidney. Bar represents mean ± s.d.

3. Discussion

We demonstrated that ω3-PUFAs significantly attenuated kidney injury by enhancing autophagy flux and inhibiting apoptosis in a renal IRI model (Fig 6). These results indicate that increasing the levels of endogenously synthesized ω3-PUFAs in the kidney may reduce the risk of IRI and attenuate oxidative stress in fat-1 transgenic mice [15]. This was associated with antioxidant effects. Furthermore, protection from renal injury in fat-1 mice correlated with the formation of UCP2 and p22phox in kidney tissue.

Oxidative stress plays an important role in the pathophysiology of IR-induced kidney injury [34]. IRI generates ROS, including hydrogen peroxide and hydroxyl radicals, known inducers of lipid peroxidation [35]. In our study, ROS and cleaved caspase-3 levels were only slightly higher in fat-1 IRI mice than in fat-1 sham mice. However, TUNEL, H&E, and PAS staining, and serum levels of creatinine were significantly greater in fat-1 IRI mice than in fat-1 sham mice. Although we cannot provide a full explanation, we suggest that ROS generation and cleaved caspase-3 levels are nearly diminished in fat-1 mice with IR renal injury. However, caspase-independent apoptosis (AIF, Endo G, HtrA2) may also be inhibited to some degree [36]. Thus, fat-1 mice do not show complete inhibition of any renal injury, as evidenced by the TUNEL staining, renal tubule-interstitial injury, and serum creatinine results. Our results suggest that fat-1 can protect against damage from oxidative stress to the kidney through regulation of UCP2 and p22phox. Accordingly, reduced ROS levels were also observed in the kidneys of fat-1 mice, leading to renoprotective effects.

Recent research has demonstrated the role of ROS in IR-induced autophagy regulation [25,37]. P62/SQSTM1 and polyubiquitinated protein aggregates may be seen as markers of autophagy function. Furthermore, p62 is a key factor that controls cell death versus survival [38]. It is an autophagy-related protein and is normally degraded by lysosomal proteases through an interaction with LC3II [38]. Its accumulation reflects the inhibition of proteasomal activity [39]. Similarly, decreased p62 levels are associated with autophagy activation. Dysregulation of autophagy can result in renal cell death, as noted in several kidney diseases. In this study, the basal level of LC3 was greater (leading to autophagy flux) in fat-1 mice than in wt mice after IRI.

Cathepsin D (a lysosomal aspartic protease) is an effector enzyme of autophagosome degradation in lysosomes, ultimately resulting in the acceleration of autophagic flux. ω3-PUFAs can directly augment cathepsin D expression in the cerebellum [31]. Moreover, they can increase lysosome activity and eventually induce proteolytic activation of cathepsin D. In addition, ATP6E expression is increased in fat-1 mice. High levels of cathepsin D and ATP6E in renal cells significantly activate autophagy flux, inducing the formation of acidic autophagic vacuoles and autophagolysosomes. Thus, ω3-PUFAs may play an important role in renoprotective effects via the activation of autophagy flux.

The energy-sensing LKB1-AMPK pathway regulates autophagy [19]. Recent studies have demonstrated that AMPK is the main initiator of stress-triggered autophagy, such as in oxidative stress, hypoxia, and nutrient deprivation [12,40]. AMPK is considered an autophagy-promoting kinase, whereas mTOR has been reported to have the opposite effect [40]. mTOR kinase is a major negative regulator of autophagy. mTOR signaling is frequently dysregulated in cancer, where LKB1/AMPK signaling can act upstream of it [20]. Our data demonstrate that ω3-PUFAs override mTOR activation induced by IRI through autophagy activation in fat-1 mice. These findings support the involvement of AMPK-mTOR signaling as an effector of the autophagy activation pathway in IRI kidneys, leading to renoprotective responses. Our fat-1 sham mice showed higher level of mTOR than wt sham mice. In our data, it is confusing that mTOR is more elevated in fat-1 sham mice that wt sham mice, unlike being decreased in fat-1 IRI mice than wt IRI mice. However, omega 3 intake increased mTOR-p70s6k signaling which control muscle protein anabolism and muscle protein growth in human [41]. It may be possible that omega 3 elevate mTOR in basal status kidney, like muscle.

This study had some limitations. Although we examined autophagy activation and the beneficial effects of ω3-PUFAs in fat-1-overexpressing IRI mice, we did not determine the beneficial effects of medication with ω3-PUFAs in IRI. Moreover, it has not been determined whether ω3-PUFAs have beneficial effects in patients with acute kidney injury.

Taken together, our results highlight for the first time that fat-1 overexpression, resulting in ω3-PUFA enrichment, helps to prevent IR-induced renal injury. This occurs via regulation of antioxidant gene expression, blocking ROS production, and repressing oxidative stress as a result of ω3-PUFA-induced autophagy activation in the kidneys of fat-1 mice versus wt mice. ω3-PUFA enrichment reduces renal cell damage, promoting autophagy flux through cathepsin D-mediated autophagy activation. Cathepsin D inhibits oxidative stress-induced cell death via activation of autophagy [42].

Peer-reviewed version available at Int. J. Mol. Sci. 2017, 18, 2081; doi:10.3390/ijms18102081

Furthermore, ω3-PUFA enrichment activates ATP6E activity, which participates significantly in renal cell survival. The present study is the first to investigate the autophagy activity of ω3-PUFAs in the kidney, in which basal autophagy in fat-1 mice was activated, and this basal autophagy activation had protective effects on renal cells through autophagy clearance-mediated ATP6E regulation. In addition, we suggest that AMPK activation by ω3-PUFA enrichment may affect overall renoprotective activity and autophagy function. These processes may underlie renal cell survival and may be potential therapeutic targets for the treatment of IRI related to renal transplantation.

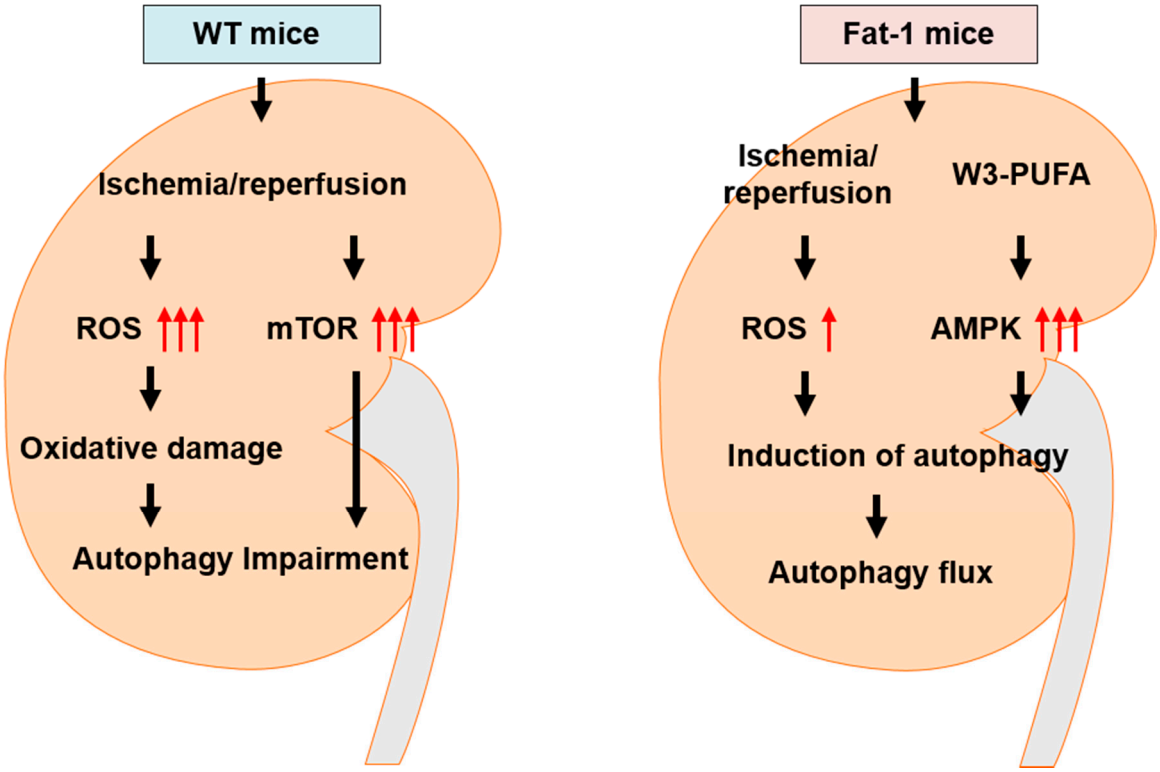

Figure 6. Schematic diagram. Ischemia-reperfusion (IR) increases kidney damage, with increased oxidative stress and less pronounced AMPK activation. Activation of AMPK inhibits reactive oxygen species-induced autophagy impairment and induces autophagy, resulting in preserved ATP content and kidney homeostasis. AMPK-mediated autophagy was reduced in wt mice damaged by IR, prompting kidney dysfunction. However, in fat-1 mice, high ω3-PUFAs increased AMPK-mediated autophagy and protected the kidney against IR via induction of autophagy and enhancement of autophagy flux.

4. Materials and Methods

4.1. Animals

Dr. J.X. Kang of Harvard Medical School (Boston, MA, USA) provided the fat-1 transgenic mice. Generations of these mice were mated to obtain heterozygous and homozygous transgenic mice. All transgenic fat-1 mice used were homozygous. The presence of the fat-1 gene in each mouse was confirmed by genotyping. Male mice were housed individually in cages on a standard 12/12 h light/dark cycle. Water and food were available ad libitum until mice were transported to the laboratory ~1 h prior to the experiments. All experiments were conducted with the approval of the Animal Care and Use Committee at Chungnam National University School of Medicine.

The mice were divided into four groups: wt sham (n = 10), fat-1 sham (n = 10), wt IR (n = 15), and fat-1 IR (n = 15). IR injury was performed as described previously [25]. Briefly, mice were anesthetized with an intraperitoneal injection of ketamine (60 mg/kg body mass) and xylazine (8 mg/kg). After an abdominal incision, both renal pedicles were clamped bluntly. During the procedure, the mouse's body temperature was kept constant at 35–36°C on a heating pad. After 35 min of ischemia, the

Peer-reviewed version available at Int. J. Mol. Sci. 2017, 18, 2081; doi:10.3390/ijms18102081

clamps were removed. Sham-treated control mice underwent a similar surgical procedure without clamping. Mice were sacrificed 24 h after the surgical procedure. Blood and kidney tissues were collected.

4.2. Blood and tissue preparation

Renal function was evaluated as described previously [2]. Blood was collected from the inferior vena cava under anesthesia at sacrifice. The blood was placed in pre-chilled microcentrifuge tubes (4°C). Serum was separated by centrifugation for 10 min at 4°C. To measure blood urea nitrogen (BUN) and serum creatinine, aliquots of serum were analyzed using a chemistry auto-analyzer, Toshiba 200FR (Toshiba Medical Systems Co., Tokyo, Japan). Tissues were prepared as described previously [2]. Briefly, the left kidney was excised immediately after sacrifice and cut into three coronal sections. Two pieces of the kidney were snap-frozen in liquid nitrogen and kept at 70°C for subsequent RNA extraction and protein analysis. The other piece of the kidney was fixed in 10% buffered formaldehyde at room temperature (RT) and then embedded in Paraplast (Sherwood Medical, St. Louis, MO, USA) for light microscopy.

4.3. Tissue injury score

Paraffin wax-embedded kidney pieces were cut into 4 μm sections and mounted on glass slides. The sections were deparaffinized with xylene, stained with hematoxylin and eosin (H&E) and PAS, and examined under a microscope (Olympus BX51, Olympus, Tokyo, Japan). Five consecutive fields were examined at ×200 magnification and tissue injury scores were averaged per slide. For PAS staining, tubular necrosis was defined as the loss of proximal tubular brush border blebbing of apical membranes or intra-luminal aggregation of cells and proteins. Tubular necrosis (injury) in PAS-stained sections was scored as follows: 0 normal, 1 < 10%, 2 10–25%, 3 26–75%, and 4 > 75%. For the H&E sections, renal cortical vacuolization, peritubular/proximal tubule leukocyte infiltration, and proximal tubule simplification were evaluated and scored as follows: normal 0, mild injury 1, moderate injury 2, and severe injury 3.

4.4. Confocal microscopy

Levels of microtubule-associated protein light chain 3 (LC3) were evaluated by confocal microscopy after immunofluorescent staining. After the end of the IR injury, the tissue was isolated and fixed in 10% formalin. Then deparaffinized sections were incubated with primary antibody overnight at 4°C. The sections were washed to remove excess primary antibody and incubated with the appropriate fluorescently labeled secondary antibodies for 1 h at RT. Nuclei were stained with DAPI for 5 min. After mounting, fluorescence images were acquired using confocal laser-scanning microscopy (LSM 700; Zeiss).

4.5. Western blot analysis

Cells were lysed in 1 mL ice-cold PRO-PREP buffer (iNtRON, Seongnam, Korea). Protein concentrations in supernatants were evaluated with a BCA protein assay kit (Thermo Scientific, South Logan, UT, USA). Aliquots of protein (30 μg/lane) were separated by 10–15% SDS PAGE and then transferred to polyvinylidene fluoride (PVDF) membranes. Membranes were blocked with blocking buffer containing 5% non-fat dry milk for 2 h at RT and then incubated with rabbit primary antibodies against actin (1:1000), LC3 (1:1000), p62 (1:1000), ATP6E (1:1000), cathepsin D (1:1000), and caspase-3 (1:500) at 4°C overnight. Membranes were washed three times with Tris-buffered saline with 0.1% Tween 20 (TTBS) for 10 min each, and then incubated with HRP-conjugated anti-rabbit IgG secondary antibodies (1:1000 each) for 2 h at RT. After washing three times in TTBS, protein bands were visualized using a chemiluminescence detection kit (Thermo Scientific, South Logan, UT, USA). The same membranes were subsequently used for β-actin immune detection, and equal protein loading was ensured.

4.6. Measurement of ROS production

ROS levels were measured using 2′,7′-dichlorofluorescein diacetate (DCFH-DA, 10 μM; Molecular Probes, Inc.) and dihydroethidium (DHE, 10 μM; Molecular Probes, Inc.), as described previously [26]. Tissues were incubated for 60 min in Krebs-HEPES buffer containing DCFH-DA and DHE and washed twice. After mounting, fluorescence images were acquired with confocal laser-scanning microscopy.

4.7. PCR

Total RNA was extracted from 30 mg tissue using the TRIzol reagent (Invitrogen, Carlsbad, USA), and PCR was performed as described previously [27]. PCR reactions were performed using Maxime PCR PreMix (Intron Biotechnology); 2 μL (10 pmol/μL) of forward and reverse primers for UCP2, p22phox, Beclin-1, Atg7, LC3, AMPK, or actin; and 1 μL cDNA template (1 μg/μL), in a total volume of 20 μL. Densitometry data for band intensities in different sets of experiments were generated by analyzing gel images with ImageJ software (ver. 1.33). Primer sequences were as follows: UCP2 (forward: 5′-CTC CCA ATG TTG CCC-3′, reverse: 5′-TGG CTT TCA GGA GAG-3′), p22phox (forward: 5′ ATTGTGGCGGGCGTGTT-3′, reverse: 5′-CGGCGGTCATGTACTTCTGTC-3′), Beclin-1 (forward: 5′-GGCCAATAAGATGGGTCTGA-3′, reverse: 5′ GCTGCACACAGTCCAGAAAA-3′), Atg7 (forward: 5′-TGCCTATGATG ATCTGTGTC-3′, reverse: 5′-CACCAACTGTTATCTTTGTCC-3′), LC3 (forward: 5′ AGCAGCATCCAACCAAAATC3′, reverse: 5′-CTGTGTCCGTTCACCAACAG-3′), AMPK (forward: 5′-AGAGGGCCGCAATAAAAGAT-3′, reverse: 5′ TGTTGTACAGGCAGCTGAGG-3′), and actin (forward: 5′ CGGTTCCGATGCCCTGAGGCTCTT-3′, reverse: 5′ CGTCACACTTCATGATGGAATTGA-3′).

4.8. TUNEL staining

Paraffin wax–embedded tissue sections were rehydrated and permeabilized using proteinase K (20 mg/mL in PBS) for 15 min at RT. Endogenous peroxidase was inactivated with 3% hydrogen peroxide in PBS. Sections were subjected to TUNEL staining using the ApopTag Peroxidase In Situ Apoptosis Detection Kit (Chemicon International, Temecula, CA) according to the manufacturer's protocol. TUNEL-positive cells were detected with fluorescent signals using an LSM5Pascal Exciter laser scanning confocal microscope. To evaluate apoptosis semi-quantitatively, five microscopic fields were selected randomly at ×200 magnification. The numbers of TUNEL-positive cells were also counted.

4.9. Autophagy analysis

Autophagosome formation was measured by LC3 punctate staining, as described previously [27]. To quantify autophagy, we used fluorescence microscopy to count the number of endogenous LC3 punctate dots in the kidney using ImageJ software. Each condition was assayed in triplicate. LC3-II protein levels were evaluated by Western blot analysis using an antibody against LC3 (Sigma Aldrich, L7543).

4.10. Statistical analysis

Data are reported as means ± SDs. Multiple comparisons among groups were performed using one-way ANOVA with a post hoc Bonferroni correction. We used SPSS software (ver. 11.0 for Windows; SPSS, Inc., Chicago, IL, USA). Differences between groups were considered significant at $P < 0.05$.

5. Conclusions

In conclusion, this study demonstrated for the first time the renoprotective effects of ω3-PUFAs, reducing ROS, by regulating antioxidant gene expression in renal cells. The renoprotective mechanism of these effects in fat-1 mice is likely related to the AMPK-mediated autophagy signaling pathway. Thus, ω3-PUFAs are candidates for renal therapy in AKI.

Acknowledgments: We thank Dr. J.X. Kang of Harvard Medical School for providing the fat-1 transgenic mice. This work was supported by the National Research Foundation of Korea (NRF) grant funded by the Korea government (MSIP) (2016R1C1B1015811) at Chungnam National University. This research was supported by Basic Science Research Program through the National Research Foundation of Korea(NRF) funded by the Ministry of Education(2010-0024594).

Author Contributions: J.J. and D.E. conceived and designed the experiments; D.H., T.W. and Y.J. performed the experiments; J.Y. and D.K. analyzed the data; K., D.W. and J.Y. contributed reagents/materials/analysis tools; J.J. and D.E. wrote the paper.

Conflicts of Interest: The authors declare no conflict of interest.

Peer-reviewed version available at Int. J. Mol. Sci. 2017, 18, 2081; doi:10.3390/ijms18102081

Abbreviations

IRI	Ischemia-Reperfusion Injury
AKI	Acute Kidney Injury
ω3-PUFAs	ω3-Polyunsaturated fatty acids
AMPK	AMP-activated protein kinase

References

1. Cooper, J.E.; Wiseman, A.C. Acute kidney injury in kidney transplantation. *Curr Opin Nephrol Hypertens.* **2013,** 22, 698-703.
2. Choi, D.E.; Jeong, J.Y.; Lim, B.J.; Chung, S.; Chang, Y.K.; Lee, S.J.; Na, K.R.; Kim, S.J.; Shin, Y.T.; Lee, K.W. Pretreatment of sildenafil attenuates ischemia-reperfusion renal injury in rats. *American journal of physiology Renal physiology*. **2009**, 297, F362-370.
3. Versteilen, A.M.; Di Maggio, F.; Leemreis, J.R.; Groeneveld, A.B.; Musters, R.J.; Sipkema P. Molecular mechanisms of acute renal failure following ischemia/reperfusion. Int J Artif Organs. 2004;27(12): 1019-1029.
4. Vercauteren SR, Ysebaert DK, Van Rompay AR, De Greef KE, De Broe ME. Acute ischemia/reperfusion injury after isogeneic kidney transplantation is mitigated in a rat model of chronic renal failure. Am J Transplant. 2003;3(5): 570-580.
5. Zweier JL, Talukder MA. The role of oxidants and free radicals in reperfusion injury. Cardiovasc Res. 2006;70(2): 181-190.
6. Yeh CH, Hsu SP, Yang CC, Chien CT, Wang NP. Hypoxic preconditioning reinforces HIF-alpha-dependent HSP70 signaling to reduce ischemic renal failure-induced renal tubular apoptosis and autophagy. Life Sci. 2010;86(3-4): 115-123.
7. Wang Z, Choi ME. Autophagy in kidney health and disease. Antioxid Redox Signal. 2014;20(3): 519-537.
8. Jiang M, Liu K, Luo J, Dong Z. Autophagy is a renoprotective mechanism during in vitro hypoxia and in vivo ischemia-reperfusion injury. Am J Pathol. 2010;176(3): 1181-1192.
9. Muhammad E, Levitas A, Singh SR, et al. PLEKHM2 mutation leads to abnormal localization of lysosomes, impaired autophagy flux and associates with recessive dilated cardiomyopathy and left ventricular noncompaction. Hum Mol Genet. 2015;24(25): 7227-7240.
10. Kandadi MR, Hu N, Ren J. ULK1 plays a critical role in AMPK-mediated myocardial autophagy and contractile dysfunction following acute alcohol challenge. Curr Pharm Des. 2013;19(27): 4874-4887.
11. Hua Y, Zhang Y, Ceylan-Isik AF, Wold LE, Nunn JM, Ren J. Chronic Akt activation accentuates aging-induced cardiac hypertrophy and myocardial contractile dysfunction: role of autophagy. Basic Res Cardiol. 2011;106(6): 1173-1191.
12. Shang L, Wang X. AMPK and mTOR coordinate the regulation of Ulk1 and mammalian autophagy initiation. Autophagy. 2011;7(8): 924-926.
13. Satriano J, Sharma K. Autophagy and metabolic changes in obesity-related chronic kidney disease. Nephrol Dial Transplant. 2013;28 Suppl 4: iv29-36.
14. Lempiainen J, Finckenberg P, Levijoki J, Mervaala E. AMPK activator AICAR ameliorates ischaemia reperfusion injury in the rat kidney. Br J Pharmacol. 2012;166(6): 1905-1915.
15. Luo C, Ren H, Wan JB, et al. Enriched endogenous omega-3 fatty acids in mice protect against global ischemia injury. J Lipid Res. 2014;55(7): 1288-1297.
16. Arterburn LM, Hall EB, Oken H. Distribution, interconversion, and dose response of n-3 fatty acids in humans. Am J Clin Nutr. 2006;83(6 Suppl): 1467S-1476S.
17. Hassan IR, Gronert K. Acute changes in dietary omega-3 and omega-6 polyunsaturated fatty acids have a pronounced impact on survival following ischemic renal injury and formation of renoprotective docosahexaenoic acid-derived protectin D1. J Immunol. 2009;182(5): 3223-3232.
18. Jing H, Yao J, Liu X, et al. Fish-oil emulsion (omega-3 polyunsaturated fatty acids) attenuates acute lung injury induced by intestinal ischemia-reperfusion through Adenosine 5'-monophosphate-activated protein kinase-sirtuin1 pathway. J Surg Res. 2014;187(1): 252-261.
19. Liang J, Shao SH, Xu ZX, et al. The energy sensing LKB1-AMPK pathway regulates p27(kip1) phosphorylation mediating the decision to enter autophagy or apoptosis. Nat Cell Biol. 2007;9(2): 218-224.

20. Son YO, Wang X, Hitron JA, et al. Cadmium induces autophagy through ROS-dependent activation of the LKB1-AMPK signaling in skin epidermal cells. Toxicol Appl Pharmacol. 2011;255(3): 287-296.
21. Alexander A, Walker CL. The role of LKB1 and AMPK in cellular responses to stress and damage. FEBS Lett. 2011;585(7): 952-957.
22. Shin S, Jing K, Jeong S, et al. The omega-3 polyunsaturated fatty acid DHA induces simultaneous apoptosis and autophagy via mitochondrial ROS-mediated Akt-mTOR signaling in prostate cancer cells expressing mutant p53. Biomed Res Int. 2013;2013: 568671.
23. Kim N, Jeong S, Jing K, et al. Docosahexaenoic Acid Induces Cell Death in Human Non-Small Cell Lung Cancer Cells by Repressing mTOR via AMPK Activation and PI3K/Akt Inhibition. Biomed Res Int. 2015;2015: 239764.
24. Menesi D, Kitajka K, Molnar E, et al. Gene and protein expression profiling of the fat-1 mouse brain. Prostaglandins Leukot Essent Fatty Acids. 2009;80(1): 33-42.
25. Gang GT, Hwang JH, Kim YH, et al. Protection of NAD(P)H:quinone oxidoreductase 1 against renal ischemia/reperfusion injury in mice. Free radical biology & medicine. 2014;67: 139-149.
26. Kim JJ, Lee HM, Shin DM, et al. Host cell autophagy activated by antibiotics is required for their effective antimycobacterial drug action. Cell Host Microbe. 2012;11(5): 457-468.
27. Yuk JM, Shin DM, Lee HM, et al. Vitamin D3 induces autophagy in human monocytes/macrophages via cathelicidin. Cell Host Microbe. 2009;6(3): 231-243.
28. Kalogeris T, Baines CP, Krenz M, Korthuis RJ. Cell biology of ischemia/reperfusion injury. Int Rev Cell Mol Biol. 2012;298: 229-317.
29. Yang CS, Yuk JM, Kim JJ, et al. Small heterodimer partner-targeting therapy inhibits systemic inflammatory responses through mitochondrial uncoupling protein 2. PloS one. 2013;8(5): e63435.
30. Huber TB, Edelstein CL, Hartleben B, et al. Emerging role of autophagy in kidney function, diseases and aging. Autophagy. 2012;8(7): 1009-1031.
31. Bak DH, Zhang E, Yi MH, et al. High omega3-polyunsaturated fatty acids in fat-1 mice prevent streptozotocin-induced Purkinje cell degeneration through BDNF-mediated autophagy. Sci Rep. 2015;5: 15465.
32. Stein SC, Woods A, Jones NA, Davison MD, Carling D. The regulation of AMP-activated protein kinase by phosphorylation. Biochem J. 2000;345 Pt 3: 437-443.
33. Lieberthal W, Fuhro R, Andry CC, et al. Rapamycin impairs recovery from acute renal failure: role of cell-cycle arrest and apoptosis of tubular cells. American journal of physiology Renal physiology. 2001;281(4): F693-706.
34. Yuan Q, Hong S, Han S, et al. Preconditioning with physiological levels of ethanol protect kidney against ischemia/reperfusion injury by modulating oxidative stress. PloS one. 2011;6(10): e25811.
35. Ozbek E. Induction of oxidative stress in kidney. Int J Nephrol. 2012;2012: 465897.
36. Kaushal GP, Basnakian AG, Shah SV. Apoptotic pathways in ischemic acute renal failure. Kidney Int. 2004;66(2): 500-506.
37. Song H, Han IY, Kim Y, et al. The NADPH oxidase inhibitor DPI can abolish hypoxia-induced apoptosis of human kidney proximal tubular epithelial cells through Bcl2 up-regulation via ERK activation without ROS reduction. Life Sci. 2015;126: 69-75.
38. Ichimura Y, Komatsu M. Selective degradation of p62 by autophagy. Semin Immunopathol. 2010;32(4): 431-436.
39. Zhang YB, Gong JL, Xing TY, Zheng SP, Ding W. Autophagy protein p62/SQSTM1 is involved in HAMLET-induced cell death by modulating apotosis in U87MG cells. Cell Death Dis. 2013;4: e550.
40. Yang CS, Kim JJ, Lee HM, et al. The AMPK-PPARGC1A pathway is required for antimicrobial host defense through activation of autophagy. Autophagy. 2014;10(5): 785-802.
41. Smith GI, Atherton P, Reeds DN, et al. Omega-3 polyunsaturated fatty acids augment the muscle protein anabolic response to hyperinsulinaemia-hyperaminoacidaemia in healthy young and middle-aged men and women. Clin Sci (Lond). 2011;121(6): 267-278.
42. Hah YS, Noh HS, Ha JH, et al. Cathepsin D inhibits oxidative stress-induced cell death via activation of autophagy in cancer cells. Cancer Lett. 2012;323(2): 208-214.